Journal of Molecular Catalysis A: Chemical 298 (2009) 74–80

Contents lists available at ScienceDirect

Journal of Molecular Catalysis A: Chemical

journal homepage: www.elsevier.com/locate/molcata

Mn(III) porphyrins immobilized on magnetic polymer nanospheres as biomimetic catalysts hydroxylating cyclohexane with molecular oxygen

Bo Fu, Han-Cheng Yu, Jin-Wang Huang*, Ping Zhao, Jie Liu, Liang-Nian Ji

MOE Key Laboratory of Bioinorganic and Synthetic Chemistry, School of Chemistry and Chemical Engineering & State Key Laboratory of Optoelectronic Material and Technologies, Sun Yat-Sen University, Guangzhou 510275, PR China

ARTICLE INFO

Article history:
Received 29 January 2008
Received in revised form 8 October 2008
Accepted 9 October 2008
Available online 17 October 2008

Keywords:
Magnetic polymer nanospheres
Mn(III) porphyrin
Hydroxylate
Cyclohexane

ABSTRACT

Three types of magnetic polymer nanospheres immobilizing Mn(III) porphyrins appending *p*-OCH_3, *p*-H and *p*-Cl phenyl substituents (designated as MPNSs(MnMP), MPNSs(MnPP) and MPNSs(MnCP), respectively) were synthesized and their catalytic activities as biomimetic catalysts to hydroxylate cyclohexane with molecular oxygen were investigated. The catalytic efficiencies of these magnetic nanospheres are much higher than those of the non-supported Mn(III) porphyrin analogues and follow the order of MPNSs(MnMP) > MPNSs(MnPP) > MPNSs(MnCP). It is also found that these nanospheres have good magnetic responsiveness and thus can be completely recovered by applying an external magnetic field. Furthermore, they can maintain their catalytic activities after being recycled several times. These results may be helpful in designing new, highly efficient metalloporphyrin catalysts.

1. Introduction

Synthetic metalloporphyrins have been extensively used as catalysts for alkene epoxidation and alkane hydroxylation under mild conditions since 1979 [1–5]. However, their use in homogeneous systems is limited by the drawbacks: the porphyrin ring is liable to oxidative self-destruction and the metalloporphyrins are subject to aggregation through π–π interaction. Immobilization of metalloporphyrins on solid supports can offer several advantages over traditional solution-phase chemistry. For example, the solid-supported metalloporphyrins have higher stability and increased selectivity. Furthermore, they can be recovered from reaction mixtures and reused. Among the supports that can be used to immobilize metalloporphyrins, polystyrene derivatives are often employed for their cheapness, ready availability, mechanical robustness, chemical inertness and facile functionalization. Moreover, they can also provide suitable microenvironment for the "accommodation" of porphyrin catalytic centers [6–11]. However, as for polystyrene supported catalysts, troublesome centrifugation or filtration is needed to recycle them. Furthermore, it causes a decrease in reaction yields and enantioselectivities [12,13]. In overcoming such problems, magnetic polymer microspheres arouse our attention due to their specific surface properties, and relatively rapid and effortless magnetic separation [14–18]. On the other hand, nanometer-sized catalyst supports have recently attracted a great deal of interest because of their high specific surface area and outstanding stability as well as activity in the liquid phase [19–24]. The combination of the easy separation of magnetic polymer microspheres and the special properties of nanometer-sized catalyst supports provides a good opportunity to design and synthesize novel polystyrene supported metalloporphyrins to mimic the function of P450 enzymes.

In this paper, a series of magnetic polymer nanospheres immobilizing Mn(III) porphyrins appending different phenyl-substituents were synthesized and characterized. The magnetic polymer nanospheres are of core/shell structure in which the core is composed of numerous Fe_3O_4 particles and the shell is composed of a copolymer of styrene and Mn(III) porphyrin acrylates. The catalytic performance of these nanospheres for cyclohexane hydroxylation with molecular oxygen was compared with that of non-supported Mn(III) porphyrin acrylates and polystyrene supported Mn(III) porphyrin. The influence of phenyl-substituents on the catalytic activity of the nanospheres was also discussed.

2. Experimental

2.1. Materials

The precursors, 5-(4-hydroxyl)phenyl-10,15,20-trimethoxyphenylporphyrin (HPTMPP), 5-(4-hydroxyl) phenyl-10,15,20-triphenylporphyrin (HPTPP) and 5-(4-hydroxyl)phenyl-10,15,20-trichlorophenylporphyrin (HPTCPP) were synthesized in our laboratory

* Corresponding author. Tel.: +86 20 84113317; fax: +86 20 84112245.
E-mail address: ceshjw@163.com (J.-W. Huang).

1381-1169/$ – see front matter © 2008 Elsevier B.V. All rights reserved.
doi:10.1016/j.molcata.2008.10.015

[25]. The magnetic fluid used in this work, Fe_3O_4 particles, was prepared by chemical coprecipitation of ferrous chloride and ferric chloride. The powder X-ray diffraction (PXRD) pattern of the Fe_3O_4 particles is available in supplementary materials (Fig. S1). The size of these particles was estimated to be *ca.* 9 nm by applying Scherrer's equation [14]. All other reagents were purchased.

2.2. Physical measurements

Elemental analysis (C, H and N) was carried out on a PerkinElmer 240 Q elemental analyzer. ESI-MS was measured on a Thermo Finnigan LCQ DECA XP spectrometer. ^{1}H NMR and ^{13}C NMR spectra were recorded on a Varian INOVA500NB superconducting Fourier transform nuclear magnetic resonance spectrometry with $CDCl_3$ as solvent at room temperature and TMS as internal standard. The powder X-ray diffraction pattern of Fe_3O_4 particles was obtained on a D/max 2200 v powder diffraction system using nickel-filtered Cu Kα X-ray source radiation. UV–Vis and IR spectra were recorded on a Shimadzu UV-3150 spectrophotometer and an Equinox 55 Fourier transformation infra-red spectrometer. The scanning electron microscopy (SEM) analyses were performed with a JSM-6330F field emission scanning electron microscope. The particle sizes were measured by a Mastersizer 2000 laser particle size analyzer. An Iris (HR) inductively coupled plasma (ICP)-atomic emission spectrometer was used to determine the contents of Mn(III) porphyrin acrylates and Fe_3O_4. Magnetic measurements were performed by using a XL-7 magnetic property measurement system. Thermal analysis was performed with a Netzsch TG-209 thermogravimetric analyzer.

2.3. Catalyst preparation

2.3.1. Synthesis of Mn(III) porphyrin acrylates

2.3.1.1. Porphyrin acrylates. Porphyrin acrylates including 5-(4-acryloxy)phenyl-10,15,20-trimethoxyphenylporphyrin (APTMPP), 5-(4-acryloxy)phenyl-10,15,20-triphenylporphyrin (APTPP) and 5-(4-acryloxy)phenyl-10,15,20-trichlorophenylporphyrin (APTCPP) were synthesized by a method similar to the procedures reported in literature [26,27]. A typical reaction was conducted as follows. A mixture of 50 mL $CHCl_3$ and 0.2500 g HPTMPP was stirred at 60 °C. 2.0 g acrylyl chloride dissolved in 5 mL $CHCl_3$ was added dropwise. After 2 h, the mixture was washed with 5% K_2CO_3 several times and then evaporated to dryness. The crude material was purified on a silica gel chromatograph using $CHCl_3$ and petroleum ether as eluent. APTMPP was obtained as a purple powder. Yield: 0.2128 g (79.2 wt%). ESI-MS [$CHCl_3$, m/z]: 775 ([APTMPP]$^+$) (Fig. S2-1). ^{1}H NMR ($CDCl_3$, 500 MHz, the assignments based on H, H-COSY and H, C-HMQC experiments, for numbering see Scheme 1): δ 8.86 (m, 8H, pyrrole ring), 8.20–8.22 (d, J = 8.5 Hz, 2H, $o_1 + o_2$), 8.08–8.10 (d, J = 8.6 Hz, 6H, $o_3 + o_4$), 7.51–7.52 (d, J = 8.5 Hz, 2H, $m_1 + m_2$), 7.22–7.24 (d, J = 8.6 Hz, 6H, $m_3 + m_4$), 6.74–6.78 (m, 1H, H_a), 6.45–6.51 (m, 1H, H_c), 6.10–6.12 (m, 1H, H_b), 4.03 (s, 9H, p-CH_3), −2.73 (s, 2H, pyrrole N–H). ^{13}C NMR (125 MHz, $CDCl_3$): δ 55.50, 112.18, 118.57, 119.73, 119.89, 120.06, 128.05, 131.18, 132.85, 134.51, 135.30, 135.55, 139.87, 150.43, 159.38, 164.64 (Fig. S3).

APTPP was similarly prepared by replacing HPTMPP by HPTPP. Yield: 76.5 wt%. ESI-MS [$CHCl_3$, m/z]: 684 ([APTPP]$^+$). (Fig. S2-2). ^{1}H NMR ($CDCl_3$, 500 MHz, the assignments based on H, H-COSY and H, C-HMQC experiments, for numbering see Scheme 1): δ 8.84–8.88 (m, 8H, pyrrole ring), 8.24–8.26 (d, J = 8.5 Hz, 2H, $o_1 + o_2$), 8.20–8.22 (d, J = 8.3 Hz, 6H, $o_3 + o_4$), 7.75 (m, 6H, $m_3 + m_4$), 7.73 (m, 3H, p), 7.53–7.54 (d, J = 8.5 Hz, 2H, $m_1 + m_2$), 6.75–6.78 (m, 1H, H_a), 6.46–6.52 (m, 1H, H_c), 6.11–6.13 (m, 1H, H_b), −2.76 (s, 2H, pyrrole N–H). ^{13}C NMR (125 MHz, $CDCl_3$): δ 118.89, 119.78, 120.23, 120.29, 126.68, 127.73, 128.07, 131.24, 132.87, 134.55, 135.32, 139.79, 142.13, 150.51, 164.65 (Fig. S4).

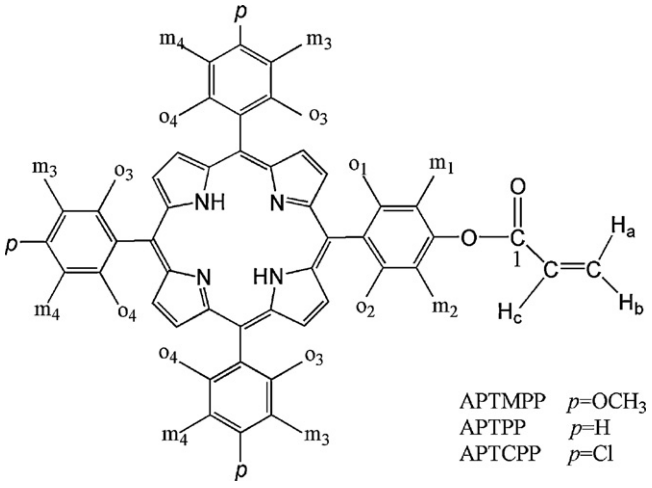

Scheme 1. Structures of APTMPP, APTPP and APTCPP.

APTCPP was also similarly prepared by replacing HPTMPP by HPTCPP. Yield: 74.3 wt%. ESI-MS [$CHCl_3$, m/z]: 788 ([APTCPP]$^+$). (Fig. S2-3). ^{1}H NMR ($CDCl_3$, 500 MHz, the assignments based on H, H-COSY and H, C-HMQC experiments, for numbering see Scheme 1): δ 8.81–8.88 (m, 8H, pyrrole ring), 8.18–8.20 (d, J = 8.6 Hz, 2H, $o_1 + o_2$), 8.09–8.10(d, J = 8.5 Hz, 6H, $o_3 + o_4$), 7.69–7.71 (d, J = 8.0 Hz, 6H, $m_3 + m_4$), 7.52–7.53 (d, J = 8.6 Hz, 2H, $m_1 + m_2$), 6.75–6.79 (m, 1H, H_a), 6.46–6.52 (m, 1H, H_c), 6.12–6.14 (m, 1H, H_b), −2.84 (s, 2H, pyrrole N–H). ^{13}C NMR (125 MHz, $CDCl_3$): δ 118.83, 118.90, 119.49, 119.87, 126.99, 128.01, 131.29, 132.96, 134.32, 135.28, 135.46, 139.43, 140.37, 150.59, 164.62 (Fig. S5).

2.3.1.2. Mn(III) porphyrin acrylates. Mn(III) porphyrin acrylates including 5-(4-acryloxy)phenyl-10,15,20-trimethoxyphenylporphyrin Mn(III) (MnAPTMPP), 5-(4-acryloxy)phenyl-10,15,20-triphenylporphyrin Mn(III) (MnAPTPP) and 5-(4-acryloxy)phenyl-10,15,20-trichlorophenylporphyrin Mn(III) (MnAPTCPP) were synthesized by a reaction of $Mn(Ac)_2$ with corresponding porphyrin acrylates. A typical reaction was conducted as follows. 0.5 g $Mn(Ac)_2$ and 1 g NaCl dissolved in 40 mL HAc were mixed with 20 mL $CHCl_3$ solution of APTMPP (0.3180 g). The mixture was stirred at 65 °C for 8 h. Then, the reaction mixture was washed with H_2O and 1 M HCl several times. After washing to neutrality with H_2O, drying over anhydrous Na_2SO_4 and concentrating *via* rotary evaporation, the residue was chromatographed on a silica gel column using $CHCl_3$ as eluent. Evaporation of solvent afforded MnAPTMPP as a green powder. Yield: 0.3427 g (96.8 wt%). (Found: C, 68.03; H, 4.38; N, 6.38%. Calc. for $C_{50}H_{36}N_4O_5MnCl{\cdot}H_2O$: C, 68.15; H, 4.35; N, 6.36%). ESI-MS [$CHCl_3$, m/z]: 827 ([MnAPTMPP]$^+$) (Fig. S2-4).

MnAPTPP, yield: 95.6 wt%. (Found: C, 71.18; H, 4.09; N, 7.03%. Calc. for $C_{47}H_{30}N_4O_2MnCl{\cdot}H_2O$: C, 71.35; H, 4.08; N, 7.08%). ESI-MS [$CHCl_3$, m/z]: 737 ([MnAPTPP]$^+$) (Fig. S2-5).

MnAPTCPP, yield: 96.8 wt%. (Found: C, 61.65; H, 3.40; N, 6.17%. Calc. for $C_{47}H_{27}N_4O_2MnCl_4{\cdot}2H_2O$: C, 61.86; H, 3.42; N, 6.14%). ESI-MS [$CHCl_3$, m/z]: 841 ([MnAPTCPP]$^+$) (Fig. S2-6).

2.3.2. Synthesis of MPNSs(MnMP), MPNSs(MnPP) and MPNSs(MnCP)

The strategy to prepare these nanospheres is shown in Scheme 2. A total of 10.0 g magnetic fluid, 12.0 g styrene,

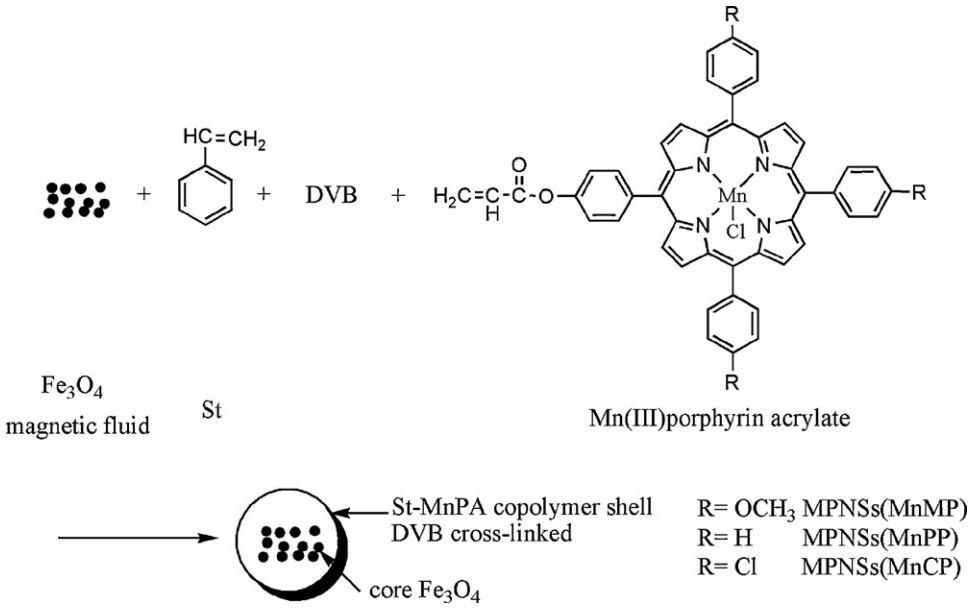

Scheme 2. The strategy to prepare MPNSs(MnMP), MPNSs(MnP) and MPNSs(MnCP).

30 mg reactive Mn(III) porphyrin acrylate, 3.0 g divinylbenzene, 1.5 g polyvinylpyrrolidone(K-30) (PVP K-30), 0.30 g 2,2′-azo-bis-isobutyronitrile (AIBN) and 100 mL H_2O/C_2H_5OH were mixed in a 250 mL round-bottomed flask equipped with a reflux condenser. The mixture was stirred at 70 °C for 20–24 h under a N_2 atmosphere. The product was washed with 1 M HCl solution to remove the unenclosed Fe_3O_4 and then with acetone to remove the residual Mn(III) porphyrin acrylate. The final product was separated by applying an additional magnetic field (0.42 T) and dried for 24 h at 60 °C in vacuum.

2.4. Catalytic experiments for cyclohexane hydroxylation

Hydroxylation of cyclohexane in the Mn(III) porphyrin–O_2–ascrobate system was carried out in a specially constructed reaction vessel at 30.0 ± 0.1 °C [6,7,27–33]. The catalytic system consists of catalyst (MPNSs(MnMP), MPNSs(MnPP), MPNSs(MnCP) or non-supported Mn(III) porphyrin acrylates), co-reductant (3.0 mmol ascrobate, 4.0×10^{-2} mmol thiosalicylic acid), substrate (5.55 mmol cyclohexane), actone/water (9:1, 10 mL) and pure oxygen (101 kPa). The products were detected by gas

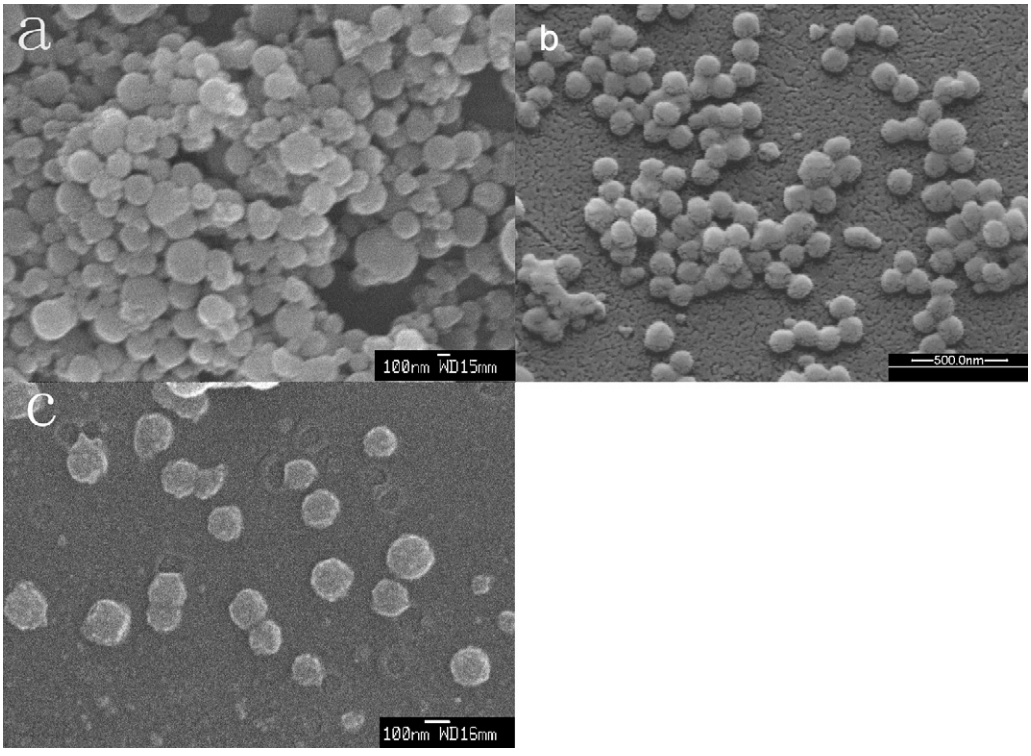

Fig. 1. SEM images of MPNSs(MnMP) (a), MPNSs(MnPP) (b) and MPNSs(MnCP) (c).

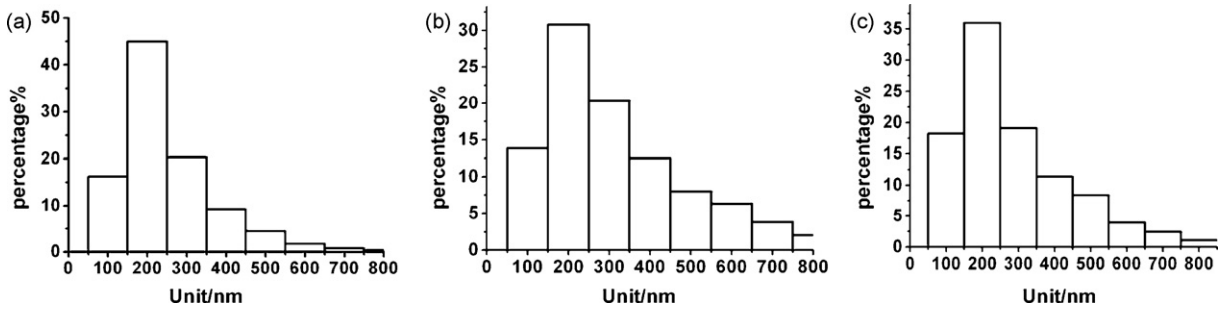

Fig. 2. Nanosphere size histograms of MPNSs(MnMP) (a), MPNSs(MnPP) (b) and MPNSs(MnCP) (c).

chromatography (GC-7890II) using *p*-chlorotoluene as internal standard.

The magnetic polymer nanospheres were recovered from the catalytic system by separating in an external magnetic field (0.42 T) after the reaction for 3 h. The hydroxylation of cyclohexane catalyzed by recovered nanospheres was performed under identical conditions.

3. Results and discussion

3.1. Characterization of magnetic microspheres

The average diameter and the surface morphology of the magnetic microspheres were obtained by SEM whose results are given in Fig. 1. The SEM images of MPNSs(MnMP), MPNSs(MnPP) and MPNSs(MnCP) (shown in Fig. 1a–c, respectively) show uniformity and spherical morphology with an average diameter of *ca.* 200 nm. The average diameter of these nanospheres is further quantitatively confirmed by the particle size analysis shown in Fig. 2.

Solid state UV–Vis spectra of these three types of nanospheres (Fig. 3) show typical Soret bands of Mn(III) porphyrin at *ca.* 480 nm and Q bands in the region of 550–650 nm. These bands have slight redshifts (about 2–3 nm) compared with those of unsupported Mn(III) porphyrin acrylates (Fig. 3, insert), indicating the existence of porphyrins in the shell.

IR spectra of these nanospheres are given in Fig. 4 and are very similar to each other. Characteristic bands of styrene and Mn(III) porphyrin acrylates are shown in the IR spectra of all these nanospheres. For example, the bands in the region of 3100–2900 cm^{-1}, three peaks at 1601, 1491 and 1446 cm^{-1} and double peaks at 758 and 700 cm^{-1} are clearly observed and can

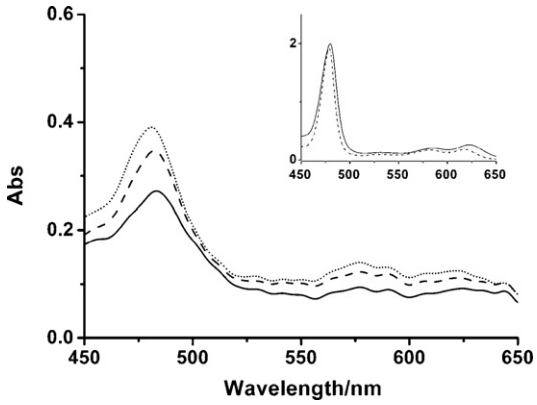

Fig. 3. Solid state UV–Vis absorption spectra of MPNSs(MnMP) (straight line), MPNSs(MnPP) (dotted line) and MPNSs(MnCP) (dashed line). Inset: absorption spectrum of Mn(III)MP (straight line), MnPP (dotted line) and MnCP (dashed line) in $CHCl_3$.

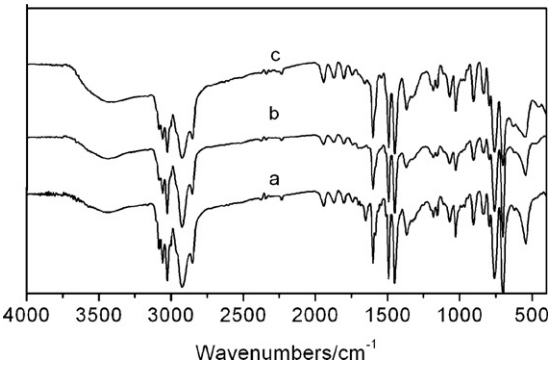

Fig. 4. IR spectra of MPNSs(MnMP) (a), MPNSs(MnPP) (b) and MPNSs(MnCP) (c).

be attributed to the benzene rings in styrene. Two peaks at 1024 and 1670 cm^{-1} attributed to the bands of C–O and C=O of Mn(III) porphyrin acrylate, respectively, are also observed. All these results suggest that the shell of the nanospheres is composed of copolymer of styrene and Mn(III) porphyrin acrylates.

Thermostabilities of the nanospheres have been determined by using thermogravimetric analysis (TGA). The TG curves (Fig. 5) give us the information that MPNSs(MnMP), MPNSs(MnPP) and MPNSs(MnCP) degrade at 262, 259 and 260 °C, respectively. This demonstrates that these catalysts are thermally stable up to almost 260 °C, exhibiting relatively high thermostabilities. The

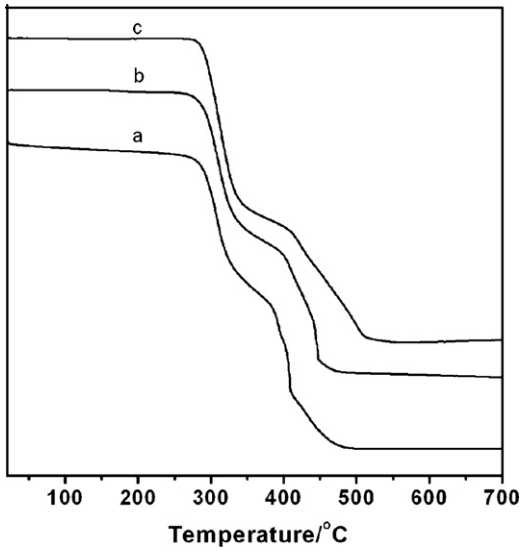

Fig. 5. TG curves of MPNSs(MnMP) (a), MPNSs(MnPP) (b) and MPNSs(MnCP) (c).

Table 1
Contents of Mn(III) porphyrin acrylates and Fe_3O_4.

Catalyst	Mn(III) porphyrin acrylate (wt%)[a]	Fe_3O_4 (wt%)
MPNSs(MnMP)	0.21%	9.10%
MPNSs(MnPP)	0.29%	11.28%
MPNSs(MnCP)	0.26%	7.29%

[a] wt% refers to the content of Mn(III) porphyrin acrylates in the nanaospheres.

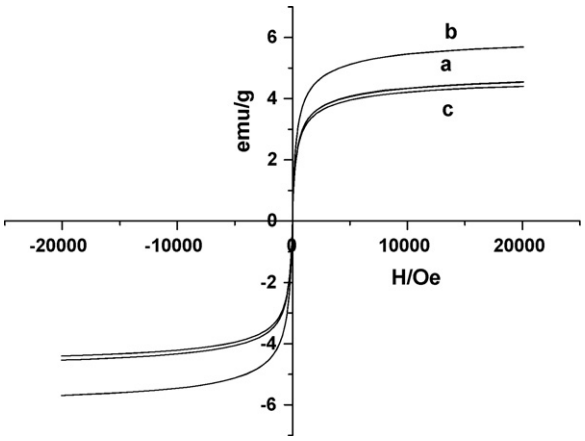

Fig. 6. Magnetic hysteresis loops of MPNSs(MnMP) (a), MPNSs(MnPP) (b) and MPNSs(MnCP) (c).

organic parts decompose completely at 485, 448, and 534 °C for MPNSs(MnMP), MPNSs(MnPP) and MPNSs(MnCP), respectively.

As is well known, one metal ion is coordinated with one porphyrin molecule. Thus, we can calculate the contents of Mn(III) porphyrin acrylates in the magnetic nanosheres from the contents of Mn which can be obtained using ICP. Using the same method, the contents of Fe_3O_4 are also calculated according to the contents of Fe in the nanospheres. The results are given in Table 1 from which we can get the quantitative information of the core and shell in the nanospheres.

These nanospheres are superparamagnetic and have excellent magnetic responsibility which is the key factor for their effortless recovery. Magnetic hysteresis loops (Fig. 6) show that all of these magnetic nanospheres exhibit superparamagnetic behavior with zero coercivity and remanence because the diameter of the magnetic Fe_3O_4 particles used in the preparation of these nanospheres is about 9 nm which is smaller than the critical particle size of Fe_3O_4 particles [34]. The saturation magnetizations of MPNSs(MnMP), MPNSs(MnPP) and MPNSs(MnCP) (4.51, 5.65 and 4.38 emu/g, respectively) are lower than that of Fe_3O_4 nanoparticles, which are due to the copolymer coating of the Fe_3O_4 nanoparticles in nanospheres [35]. Furthermore, it was experimentally observed that these nanospheres dispersed in water are rapidly attracted (<1 min) by a conventional magnet placed close to the reaction vessel (Fig. 7), demonstrating the efficacy of magnetic separation.

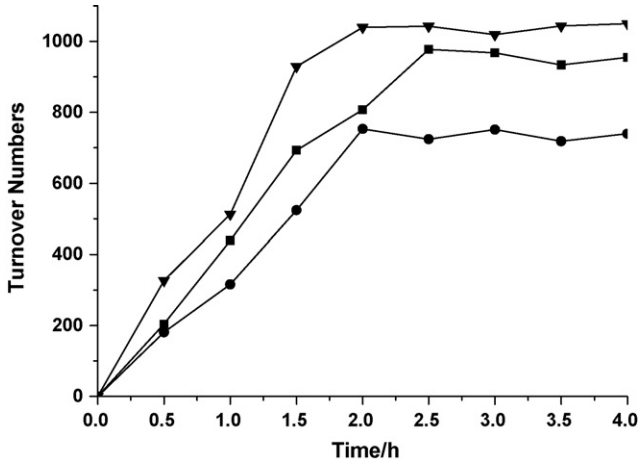

Fig. 8. Changes of the turnover numbers of MPNSs(MnMP) (▼), MPNSs(MnPP) (■) and MPNSs(MnCP) (●) calculated from the reaction products with catalytic time.

3.2. Hydroxylation of cyclohexane catalyzed by Mn(III) porphyrins immobilized on magnetic polymer nanospheres

The hydroxylation of cyclohexane catalyzed by these nanospheres was investigated in the Mn(III) porphyrin–O_2–ascrobate system. Usually cyclohexanol and cyclohexanone are the main products of the oxidation of cyclohexane in the matelloporphyrin–O_2–ascrobate system under mild conditions [6,7,26–32]. The kinetic curves of turnover numbers for MPNSs(MnMP), MPNSs(MnPP) and MPNSs(MnCP) are shown in Fig. 8, from which we can find that the curves have a similar trend, enhancing rapidly and reaching maximum values after about 3 h. The turnover numbers are unchanged with a further increase in the reaction time. These results further suggest that the by-products which come from the over-oxidation of cyclohexanol and cyclohexanone in our reaction system are negligible and 3 h may be the optimum reaction time in the experiments of cyclohexane hydroxylation catalyzed by these catalysts.

The results of cyclohexane hydroxylation catalyzed by these nanospheres (fresh and recovered) and non-supported Mn(III) porphyrin acrylates after reaction for 3 h are listed in Table 2. Controlled experiments using styrene-acrylic acid copolymer microspheres as catalysts were carried out and did not lead to substantial product yields (data not shown). From Table 2, we can easily find that the three types of nanospheres all have much higher catalytic activities than non-supported Mn(III) porphyrin acrylates. The total turnover numbers of the nanospheres are

Fig. 7. Illustration of the magnetic separation of MPNSs(MnMP) (a), MPNSs(MnPP) (b) and MPNSs(MnCP) (c) from the liquid media.

Table 2
The catalytic performance of MPNSs(MnMP), MPNSs(MnPP), MPNSs(MnCP) and Mn(III) porphyrin acrylates to hydroxylate cyclohexane after reaction for 3 h.

Catalysts[a]	Run	Product amount/μmol (turnover number[b])		
		Cyclohexanol	Cyclohexanone	Total
MPNSs(MnMP)	1	57.9(729)	23.2(288)	81.1(1017)
	2	59.3(742)	25.4(317)	84.7(1059)
	3	57.9(729)	23.7(296)	81.6(1025)
	4	58.5(731)	23.9(299)	82.4(1030)
	5	59.2(740)	24.9(310)	84.1(1050)
MPNSs(MnPP)	1	55.2(709)	16.4(211)	71.6(920)
	2	54.0(693)	17.8(229)	71.8(922)
	3	57.0(732)	16.8(216)	73.8(949)
	4	57.6(740)	14.6(187)	72.2(928)
	5	63.2(812)	10.3(133)	73.5(945)
MPNSs(MnCP)	1	43.2(540)	15.1(189)	58.3(729)
	2	44.2(552)	15.4(192)	59.6(744)
	3	42.6(533)	17.3(216)	59.9(749)
	4	42.7(534)	17.6(220)	60.3(754)
	5	41.1(514)	18.0(226)	59.1(740)
Mn(III) porphyrin acrylate	1	3.14(2.43)	1.31(1.01)	4.45(3.44)

[a] Mn(III) porphyrin in the nanospheres and non-supported Mn(III) porphyrin acrylates is 0.08 and 1.29 μmol, respectively.
[b] Turnover number = product (mol)/catalyst (mol).

about 215–308 times larger than those of non-supported Mn(III) porphyrin acrylates. As is well known, the hydrophobic microenvironment produced by the protein chain folded around the binding site of cytochrome P450 plays an important role in the process of hydroxylating substrate [6]. However, metalloporphyrins as models of cytochrome P450 have limited catalytic activities to hydroxylate substrate under mild conditions, which may be caused by the lack of this hydrophobic microenvironment. It is believed that the nanospheres provide suitable microenvironment for the "accommodation" of porphyrin catalytic centers [6–11] and thus remarkably enhance the catalytic capability of Mn(III) porphyrins.

Moreover, it is notable that the catalysis of these magnetic nanospheres to hydroxylate cyclohexane with molecular oxygen is also more effective than that of other polystyrene-supported metalloporphyrins whose sizes are about 30–60 mesh under identical mild conditions [7,8,28]. The total turnover numbers of MPNSs(MnMP), MPNSs(MnPP) and MPNSs(MnCP) are 54–78 folds larger than that of polystyrene-supported Mn(III) porphyrin which we reported previously [8]. It seems that the enhanced activities of these nanospheres are related to the high specific surface area of them. The hydrophobic microenvironment on the surface of nanospheres may also play a significant role in accelerating hydroxylation by constructing a reaction field based on the spatial interaction with substrate molecules [36].

Interestingly, the turnover numbers of the three types of nanospheres under identical conditions follow the order of MPNSs(MnMP) > MPNSs(MnPP) > MPNSs(MnCP) (Table 2 and Fig. 8). We believe that the difference in catalytic activity among these magnetic nanospheres is caused by the difference of the phenyl substituents on the porphyrin core. We have reported the substituent effect of non-supported metalloporphyrins on their biomimetic catalysis with molecular oxygen [29]. Usually, existence of electron-donating phenyl substituents in the meso position of porphyrin, such as $-OCH_3$, will increase the electron density of center metal ions. According to the theory about the catalytic cycle of cytochrome P450 [6], the increase in electron density of the center metal ion in metalloporphyrin is in favor of reduction of the metal ion, and coordination and activation of dioxygen as well as formation of active intermediate hypervalent metal–oxo species, and thus leads to high catalytic activity of metalloporphyrin. Apparently, the substituent effect also exists in the catalytic process of magnetic nanospheres and the nanospheres with electron-donating *p*-OCH_3 on porphyrin are more efficient catalysts than those with electron-withdrawing *p*-Cl groups. This result is well consistent with our previous report [29].

It is notable that these catalysts can be completely recovered and effectively reused although they are nano-sized. As shown in Table 2, these catalysts retain their high turnover numbers after being reused five times. There is no loss of magnetic responsiveness or morphological change after recycle. Meanwhile, the UV–Vis and IR spectra of these recovered nanospheres did not show any substantial change compared with those of the fresh ones. The results above provide strong evidence for the stable catalytic capabilities and chemical properties of these catalysts.

On the basis of these data, we propose that these magnetic nanospheres immobilizing Mn(III) porphyrin are excellent potential candidates for recoverable and reusable catalysts to model P450 enzymes, irrespective of their substituents. MPNSs(MnMP) are the ideal ones in the system we studied since the *p*-OCH_3 group on the porphyrin enhances the catalytic activity of this type of nanospheres.

4. Conclusions

We have prepared three types of novel magnetic polymer nanospheres immobilizing Mn(III) porphyrin appending different phenyl substituents and have investigated their catalysis to hydroxylate cyclohexane. These core/shell structured nanospheres are of an average diameter of *ca.* 200 nm and have good magnetic responsiveness. The turnover numbers of these nanospheres to hydroxylate cyclohexane are much larger than those of non-supported Mn(III) porphyrin acrylates or other polystyrene-supported Mn(III) porphyrins under identical conditions and follow the order of MPNSs(MnMP) > MPNSs(MnPP) > MPNSs(MnCP). Electron-donating groups on the periphery of porphyrins can enhance the catalytic activity of the nanospheres. Moreover, these magnetic nanospheres can be effectively recovered and can retain their high catalytic activity after being recycled five times. These results may facilitate the design of new, highly efficient metalloporphyrin catalysts.

Acknowledgments

We are grateful to the supports of Guangzhou Municipality Science & Technology Bureau of China, the National Natural Science Foundation of China and National Key Foundation Research Development Project (973) Item of China (No. 2007 CB815306).

Appendix A. Supplementary data

Supplementary data associated with this article can be found, in the online version, at doi:10.1016/j.molcata.2008.10.015.

References

[1] W. Nam, S.E. Park, I.K. Lim, M.H. Lim, J. Hong, J. Kim, J. Am. Chem. Soc. 125 (2003) 14674–14675.
[2] I. Tabushi, N. Koga, J. Am. Chem. Soc. 101 (1979) 6456–6458.
[3] T. Groves, T.E. Nemo, R.S. Myers, J. Am. Chem. Soc. 101 (1979) 1032–1033.
[4] D. Mansuy, Pure Appl. Chem. 6 (1987) 759–770.
[5] B. Meunier, Chem. Rev. 92 (1992) 1411–1456.
[6] D. Mansuy, C.R. Chim. 10 (2007) 392–413.
[7] Z.L. Liu, J.W. Huang, L.N. Ji, J. Mol. Catal. A: Chem. 104 (1996) 193–196.
[8] J.W. Huang, W.J. Mei, J. Liu, L.N. Ji, J. Mol. Catal. A: Chem. 170 (2001) 261–265.
[9] N.E. Leadbeater, M. Marco, Chem. Rev. 102 (2002) 3217–3274.
[10] V. Mirkhani, M. Moghadam, S. Tangestaninejad, H. Kargar, Appl. Catal. A: Gen. 303 (2006) 221–229.
[11] S. Berner, S. Biela, G. Ledung, A. Gogoll, J.E. Bäckvall, C. Puglia, S. Oscarsson, J. Catal. 244 (2006) 86–91.
[12] I.F.J. Vankerlecom, D. Tas, R.F. Rartan, V.V. deVyver, P.A. Jacobs, Angew. Chem. Int. Ed. Engl. 35 (1996) 1346–1348.
[13] X.Y. Liu, X.B. Ding, Z.H. Zheng, Y.X. Peng, X.P. Long, X.C. Wang, A.S.C. Chan, C.W. Yip, J. Appl. Polym. Sci. 90 (2003) 1879–1884.
[14] T. Valdés-Solís, P. Valle-Vigón, M. Sevilla, A.B. Fuertes, J. Catal. 251 (2007) 239–243.
[15] J.H. Zhang, X.B. Ding, Y.X. Peng, M. Wang, J. Appl. Polym. Sci. 90 (2003) 1879–1884.
[16] X. Ding, W. Li, Z. Zheng, J. Deng, A.S.C. Chan, P. Li, J. Appl. Polym. Sci. 79 (2001) 1847–1851.
[17] H. Noguchi, N. Yanase, Y. Uchida, T. Suzuta, J. Appl. Polym. Sci. 48 (1993) 1539–1547.
[18] A. Garcia, J. Clin. Microbiol. 37 (1999) 709–714.
[19] Y. Jiang, Q. Gao, J. Am. Chem. Soc. 128 (2006) 716–717.
[20] B. Yoon, C.M. Wai, J. Am. Chem. Soc. 127 (2005) 17174–17175.
[21] G. Korneva, H. Ye, Y. Gogotsi, D. Halverson, G. Friedman, J.-C. Bradley, K.G. Kornev, Nano Lett. 5 (2005) 879–884.
[22] S. Ko, J. Jang, Angew. Chem. Int. Ed. 45 (2006) 7564–7567.
[23] A.H. Lu, W. Schmidt, N. Matoussevitch, H. Bknnemann, B. Spliethoff, B. Tesche, E. Bill, W. Kiefer, F. SchLth, Angew. Chem. Int. Ed. 43 (2004) 4303–4306.
[24] S.C. Tsang, V. Caps, I. Paraskevas, D. Chadwick, D. Thompsett, Angew. Chem. Int. Ed. 43 (2004) 5645–5649.
[25] J.W. Huang, J.F. Liu, X.D. Jiao, L.N. Ji, Chem. J. Chin. Univ. 16 (1995) 163–167.
[26] E. Hasegawa, J. Nemoto, T. Kanayama, E. Tsuchida, Eur. Polym. J. 14 (1978) 123–127.
[27] H.C. Yu, X.L. Chen, X.X. Li, J.W. Huang, L.N. Ji, Front. Chem. Eng. China 1 (2007) 65–67.
[28] W.J. Mei, J.W. Huang, S.G. Hu, L.N. Ji, Acta Sci. Nat. Unvis. Sun Yet-Sen 39 (2000) 125–126.
[29] L.N. Ji, M. Liu, A.K. Hsieh, T.S.A. Hor, J. Mol. Catal. 70 (1991) 247–257.
[30] Q.Z. Ren, J.W. Huang, Z.L. Liu, G.T. Luo, L.N. Ji, S. Afr. J. Chem. 50 (1997) 181–183.
[31] Q.Z. Ren, J.W. Huang, X.B. Peng, L.N. Ji, J. Mol. Catal. A: Chem. 148 (1999) 9–16.
[32] J.W. Huang, W.Z. Huang, W.J. Mei, J. Liu, S.G. Hu, L.N. Ji, J. Mol. Catal. A: Chem. 156 (2000) 275–278.
[33] Q.Z. Ren, Z.A. Zhu, J.W. Huang, L.N. Ji, Y.T. Chen, J. Porphyrins Phthalocyan. 5 (2001) 449–455.
[34] J. Lee, T. Isobe, M. Senna, J. Colloid Interface Sci. 177 (1996) 490–494.
[35] S. Santra, R. Tapec, N. Theodoropoulou, J. Dobson, A. Hebard, W. Tan, Langmuir 17 (2001) 2900–2906.
[36] H. Kameyama, F. Narumi, T. Hattori, H. Kameyama, J. Mol. Catal. A: Chem. 258 (2006) 172–177.